Astronomy & Astrophysics manuscript no. m31_rednova
August 6, 2018

Letter to the Editor

The January 2015 outburst of a red nova in M31

Alexander Kurtenkov[1,8], Peter Pessev[2,7], Toma Tomov[3], Elena A. Barsukova[4], Sergei Fabrika[4,15], Krisztián Vida[5], Kamil Hornoch[6], Evgeni P. Ovcharov[1], Vitaly P. Goranskij[9], Azamat F. Valeev[4,15], László Molnár[5], Krisztián Sárneczky[5], Andon Kostov[8], Petko Nedialkov[1], Stefano Valenti[10], Stefan Geier[2,7], Klaas Wiersema[11], Martin Henze[12,16], Allen W. Shafter[13], Rosa Victoria Muñoz Dimitrova[8], Vasil N. Popov[8], and Maximilian Stritzinger[14]

1. Department of Astronomy, University of Sofia, 5 James Bourchier Blvd., 1164 Sofia, Bulgaria, `al.kurtenkov[at]gmail.com`
2. Instituto de Astrofísica de Canarias, 38200 La Laguna, Tenerife, Spain, `peter.pessev[at]gtc.iac.es`
3. Centre for Astronomy, Faculty of Physics, Astronomy and Informatics, Nicolaus Copernicus University, Grudziadzka 5, 87-100 Torun, Poland, `tomov[at]umk.pl`
4. Special Astrophysical Observatory, Nizhnij Arkhyz, Russia
5. Konkoly Observatory, Hungarian Academy of Sciences, H-1121 Budapest, Konkoly Thege Miklós út 15-17, Hungary
6. Astronomical Institute, Academy of Sciences, CZ-251 65 Ondřejov, Czech Republic
7. Departamento de Astrofísica, Universidad de La Laguna, E-38206 La Laguna, Tenerife, Spain
8. Institute of Astronomy and NAO, Bulgarian Academy of Sciences, 72 Tsarigradsko Chaussee Blvd., 1784 Sofia, Bulgaria
9. Sternberg Astronomical Institute, M.V. Lomonosov Moscow State University, Universitetskii pr. 13, 119992 Moscow, Russia
10. Las Cumbres Observatory Global Telescope Network, 6740 Cortona Dr., Suite 102, Goleta, CA 93117, USA
11. Department of Physics and Astronomy, University of Leicester, Leicester, LE1 7RH, UK
12. European Space Astronomy Centre, P.O. Box 78, 28692 Villanueva de la Cañada, Madrid, Spain
13. Department of Astronomy, San Diego State University, San Diego, CA 92182, USA
14. Department of Physics and Astronomy, Aarhus University, Ny Munkegade 120, DK-8000 Aarhus C, Denmark
15. Kazan Federal University, Kazan, 420008, Russia
16. Institut de Ciències de l'Espai (CSIC-IEEC), Campus UAB, C/Can Magrans s/n, E-08193 Cerdanyola del Valles, Spain

Received May 20, 2015; accepted May 28, 2015

ABSTRACT

Context. M31N 2015-01a (or M31LRN 2015) is a red nova that erupted in January 2015 – the first event of this kind observed in M31 since 1988. Very few similar events have been confirmed as of 2015. Most of them are considered to be products of stellar mergers.
Aims. Results of an extensive optical monitoring of the transient in the period January-March 2015 are presented.
Methods. Eight optical telescopes were used for imaging. Spectra were obtained on BTA, GTC and the Rozhen 2m telescope.
Results. We present a highly accurate 70 d lightcurve and astrometry with a 0.05″uncertainty. The color indices reached a minimum 2-3 d before peak brightness and rapidly increased afterwards. The spectral type changed from F5I to F0I in 6 d before the maximum and then to K3I in the next 30 d. The luminosity of the transient was estimated to $8.7^{+3.3}_{-2.2} \times 10^5 L_\odot$ during the optical maximum.
Conclusions. Both the photometric and the spectroscopic results confirm that the object is a red nova, similar to V838 Monocerotis.

Key words. stars: novae, cataclysmic variables – stars: individual (M31N 2015-01a, M31-RV, V838 Mon, V1309 Sco, V4332 Sgr)

1. Introduction

Red novae (or red transients) are a rare class of optical transients, reaching a peak luminosity equal to or higher than the brightest classical novae, but still lower than supernovae. Many of them are best explained by binary star mergers (Tylenda & Soker 2006) and therefore are often referred to as stellar mergers or "mergebursts" (Tylenda et al. 2011; Kochanek et al. 2014). Common observational properties during the first months of the outburst are the initial slow decline and a spectrum changing towards a late-type supergiant phase with colors shifting to the red.

Modern observational history of these events goes back to 1988 when the transient M31-RV was detected by Rich et al. (1989) as an M0 supergiant variable with peak absolute $M_{bol} \sim -10$. A similar outburst in the Milky Way was observed in 1994 – V4332 Sgr changed its spectrum from K3 to M8-9 during a 3-month period (Martini et al. 1999). The eruption of V838 Mon in February 2002 (Munari et al. 2002) reached an apparent magnitude of V=6.7 mag and was studied quite closely. The lightcurve showed three maxima and a consistent change of colors redwards as the spectrum reached an L supergiant phase at the end of the year (Evans et al. 2003). The resulting circumstellar light echo was used to obtain a distance estimate of 6.1±0.6 kpc, corresponding to a peak absolute magnitude $M_V = -9.8$ (Bond et al. 2003; Sparks et al. 2008). A bright (peak $M_R \sim -12$) event, M85 OT2006-1, was reported by Kulkarni et al. (2007). Like other red novae, it showed a narrow Hα emission, a temperature decrease and an infrared excess a few months after the eruption (Rau et al. 2007).

V1309 Sco is another Milky Way red nova, discovered in 2008. Tylenda et al. (2011) have shown that the progenitor is a contact binary with a 1.4-day period, thereby adding a significant argument in favour of the stellar merger model for the cause of these outbursts.

It has been suggested that the first catalogued nova, CK Vul was also a "red transient" (Kaminski et al. 2015). A possible red nova in M101 was reported by Goranskij et al. (2015).

Table 1. Telescopes used for the monitoring of M31N 2015-01a. The last column contains the designations used in the online Table 4.

Telescope	Observatory	Country	Image scale [arcsec/px]	Des.
6 m BTA	SAO RAS	Russia	0.36	BTA
2.5 m NOT	ORM	Spain	0.19	NOT
2 m RCC	Rozhen NAO	Bulgaria	0.74	R2M
1 m LCOGT	McDonald	USA	0.47	LCOGT
65 cm	Ondřejov	Czech Rep.	1.05	ONDR
60/90 cm Schmidt	Konkoly	Hungary	1.03	KSCH
50/70 cm Schmidt	Rozhen NAO	Bulgaria	1.08	RSCH
50 cm Cassegrain	Uni Leicester	UK	0.89	UL50

Here, we present a new addition to this class of objects, a red nova that erupted in M31 in Jan 2015. M31N 2015-01a was discovered by the MASTER-Kislovodsk auto-detection system on 2015 Jan 13 at ~19.0 mag, unfiltered (Shumkov et al. 2015). It was incorrectly identified as a classical nova by Kurtenkov et al. (2015a) based on a strong Hα emission on the Jan 16 spectrum, also reported by Hodgkin et al. (2015). On Jan 15 the object showed the spectral characteristics of an F5 supergiant (Fabrika et al. 2015). The transient became very bright, reaching a peak magnitude of R~15.1 mag circa Jan 22. It then proceeded to fade slowly and consistently turned redder. At the end of February the colors had changed considerably with the spectrum resembling that of a K supergiant. Subsequently, we announced that the transient is a red nova (Kurtenkov et al. 2015b). Our supposition that the overall spectral evolution of the object is very similar to the observed in V838 Mon was confirmed by Williams et al. (2015, Fig. 2). The possible progenitor system has been discussed by Dong et al. (2015) and Williams et al. (2015).

2. Observations and data reduction

We performed imaging of M31N 2015-01a in Johnson-Cousins *BVRI* filters (Table 1). The science frames were divided by flat fields after dark/bias subtraction.

Images of vastly different depths and FOVs were obtained. In order to do all the photometry in a similar manner, we used four bright reference stars, within 1.6′ from the transient (Table 2). That way systematic effects over large FOVs are not affecting the results. This also allowed us to minimize the instrumental errors of the references. Three out of those four stars were used for each frame. Massey et al. (2006) found systematic differences of the order of 0.1 mag between their magnitudes and the ones by Magnier et al. (1992), so we used the Massey catalog to recalibrate the *BVRI* magnitudes of the four references. Two images per filter and between 18 and 30 stars per image were used for the recalibration. The peak signals of the four reference stars on those images are within the linear range of the detector. The results are presented in Table 2.

Aperture photometry was done for all individual frames. The aperture radii we used were in the range of 1–1.5 FWHM of the Gaussian profiles of point sources. The results are presented as online material in Table 4. Only the mean JD and median magnitude are given where several consecutive images are available.

Spectra of M31N 2015-01a were obtained with three telescopes – the 6 m BTA at SAO RAS, the 10.4 m GTC at ORM and the 2 m RCC telescope at Rozhen NAO (Table 3). All the data reduction and calibrations were carried out with standard MIDAS[1] (BTA) and IRAF[2] (2m RCC and GTC) procedures. The BTA and the GTC spectra were calibrated in relative fluxes using spectrophotometric standards G191-B2B, Hiltner 600 and Hz 2 (Oke 1990; Hamuy et al. 1992, 1994).

Table 2. List of reference stars. The magnitudes are calibrated by the Massey et al. (2006) catalog using images from the 6m BTA, the Rozhen 2m and the Konkoly Schmidt telescopes.

α (J2000)	δ (J2000)	B	V	R	I
00:42:08.9	+40:55:33	14.521	13.739	13.312	12.886
00:42:12.6	+40:54:38	14.792	14.267	13.996	13.699
00:42:12.2	+40:55:49	16.030	15.287	14.883	14.495
00:42:05.3	+40:53:38	16.876	15.915	15.381	14.822
rms of calibration:		0.015	0.007	0.008	0.015

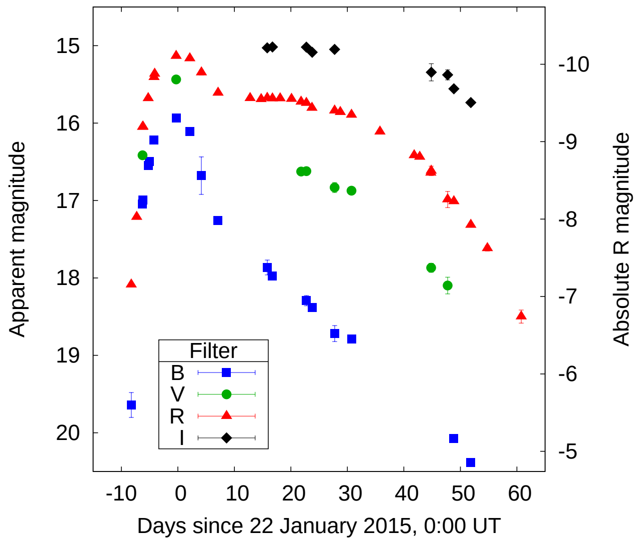

Fig. 1. Lightcurve of M31N 2015-01a in Johnson-Cousins *BVRI* filters. The zero-point moment roughly coincides with the *R*-band peak. The absolute magnitude scale (right) applies to the *R*-band datapoints only.

Table 3. Log of spectral observations. The instruments are described by Jockers et al. (2000), Afanasiev & Moiseev (2005) and Cepa (1998).

Date	Telescope/Instrument	R	Range [Å]	Exp. time [s]
Jan 15	BTA/SCORPIO	1000	4050-5850	1500
Jan 16	2mRCC/FoReRo2	400	5500-7500	4×900
Jan 17	2mRCC/FoReRo2	400	5500-7500	5×900
Jan 21	BTA/SCORPIO	1000	4050-5850	1800
Feb 21	BTA/SCORPIO	1000	3720-5530	2700
Feb 22	BTA/SCORPIO	1000	5750-7500	1800
Feb 24	GTC/OSIRIS	2500	4430-9090	6×180

3. Results and discussion

3.1. Astrometry

Astrometric calibrations were made using both the PPMXL (Roeser et al. 2010) and the LGGS (Massey et al. 2006) cata-

[1] See http://www.eso.org/sci/software/esomidas/

[2] IRAF is distributed by the National Optical Astronomy Observatory, which is operated by the Association of Universities for Research in Astronomy (AURA) under a cooperative agreement with the National Science Foundation.

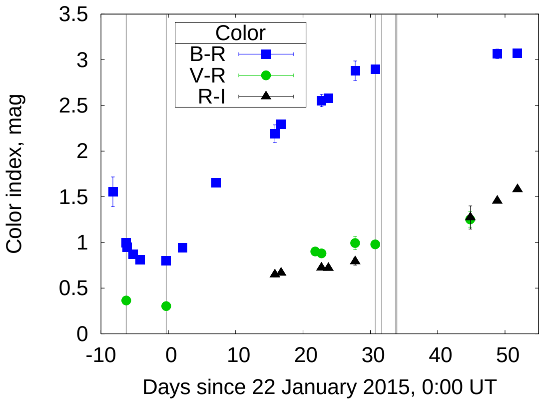

Fig. 2. The change of the observed color indices. Vertical lines represent the times the BTA (thin) and GTC (thick) spectra were taken at.

logs. Astrometric solutions were obtained for 5 images from the 10.4 m GTC, 6 m BTA and 1 m LCOGT telescopes with an atmospheric seeing in the range of 1.3″ – 1.7″. Separate calibrations were made using 20 relatively bright stars from the PPMXL catalog and 16 fainter stars close to the transient from LGGS. From PPMXL we derived α, δ (J2000) = $00^h42^m08^s.053$, $+40°55'01''.27$ with uncertainties of $\Delta_\alpha \sim 0.2''$, $\Delta_\delta \sim 0.1''$. The LGGS calibrations yielded α, δ (J2000) = $00^h42^m08^s.065$, $+40°55'01''.33$ with $\Delta_\alpha \sim \Delta_\delta \sim 0.05''$.

3.2. Photometry

The light curve of M31N 2015-01a (Fig. 1) shows a distinct similarity to the V1309 Sco lightcurve during the first month of the outburst (Mason et al. 2010). The Jan 21 datapoints are obtained shortly after the *B*-band and before the *R*-band maxima, so we assume that they coincide with the *V*-band maximum at 15.43 mag. The initial fading has been quite slow. The decline times by 2 mag after the maximum t_2 were $\sim 17\,d$, $\sim 40\,d$ and $\sim 50\,d$ in *B*, *V* and *R*-bands respectively. The colors have been consistently shifting to the red, e.g. $B-R$ increased by 2.1 mag in the 31 days after the maximum. The *R* magnitude reached a plateau 0.6 mag below the maximum in ~10 d, but no rebrightening followed, as was the case with V838 Mon.

Figure 2 shows the change of colors. The color temperature initially increased and reached a peak 2–3 d before the *R*-band maximum. Afterwards it has consistently decreased as the $B-R$ index increased by ~2 mag in one month.

3.3. Spectroscopy

The aim of the FoReRo2 spectra of M31N 2015-01a obtained 5 and 4 days before the maximum was to confirm that the object is a nova. The only features in these spectra are the emission lines of Hα with equivalent widths 19 ± 1 Å and 17 ± 1 Å on Jan 16 and 17 respectively and a Na I doublet absorption. After a careful re-calibration of the wavelength scales (see Kurtenkov et al. 2015a) the measured radial velocities of the Hα emission peaks are $-365\,\mathrm{km\,s^{-1}}$ and $-350\,\mathrm{km\,s^{-1}}$. In good agreement with the velocity of $\sim -370 \pm 50\,\mathrm{km\,s^{-1}}$ estimated by Fabrika et al. (2015) for the part of M31 where the object is located.

The first SCORPIO spectrum was obtained 6 days before the maximum brightness. The spectral region covered (4050-5850 Å) is dominated by absorption lines of ionized and neutral elements like Fe II, Ti II, Cr II, Mg II and Fe I. Hγ and Hδ are visible in absorption, while Hβ absorption is partially filled by an emission component. A comparison of the absorption line spectrum with the Jacoby et al. (1984) library of stellar spectra shows very close similarity with a F5I spectrum. The next SCORPIO spectrum obtained on Jan 21 more or less coincides with the brightness maximum. The absorption line spectrum remained practically the same. However, the continuum is much bluer (Fig. 3) showing a better resemblance with a F0I spectrum. We cross-correlated these two spectra with a F5I template and found a radial velocity for the pre-maximum spectrum $-462 \pm 38\,\mathrm{km\,s^{-1}}$ and $-534 \pm 14\,\mathrm{km\,s^{-1}}$ for the spectrum around brightness maximum (measured using the IRAF FXCOR package). The cross-correlation of the M31N 2015-01a spectra itself, confirms a velocity difference of $64 \pm 13\,\mathrm{km\,s^{-1}}$. Taking into consideration the velocity $-370\,\mathrm{km\,s^{-1}}$, connected with M31, we found that the heliocentric velocity of the ejected matter on Jan 15 was $\sim 90\,\mathrm{km\,s^{-1}}$ and increased to $\sim 160\,\mathrm{km\,s^{-1}}$ on Jan 21.

One month after the maximum we obtained two additional SCORPIO spectra in consecutive nights and one OSIRIS spectrum two days later. At that time the V brightness of the star decreased by ~1.5 mag and the colors drastically reddened. Correspondingly, the spectrum of M31N 2015-01a moved to the lower temperature classes. Now, the neutral elements absorptions dominate the spectrum together with weak TiO molecular bands. Among the strongest absorptions in the spectrum are the Na I doublet, Ba II 6142 Å and 6497 Å Ca I 6573 Å confirmed by Williams et al. (2015), and the near IR triplet of Ca II. The Ca II H & K lines are detected in emission. The strong Na I lines are well split in our OSIRIS spectrum. This allowed us to estimate their FWHM~ $200 \pm 15\,\mathrm{km\,s^{-1}}$ and their radial velocity to $\sim -570 \pm 15\,\mathrm{km\,s^{-1}}$. In good accordance with the velocity measured in all our February spectra of M31N 2015-01a (see below) and testifies to the stellar origin of these absorptions. In the OSIRIS spectrum Hα presents as a very weak emission divided in two components by a central absorption. In the SCORPIO spectrum only a marginal emission component can be seen. A comparison of the M31N 2015-01a spectrum about one month after the brightness maximum with the stellar spectra libraries of Jacoby et al. (1984) and Le Borgne et al. (2003) shows closest similarity with a K3-4I spectral type. Cross-correlating the February spectra with a K3I template we estimated an average velocity $-588 \pm 40\,\mathrm{km\,s^{-1}}$, suggesting an increase of the ejected matter velocity to $\sim 220\,\mathrm{km\,s^{-1}}$. The cross-correlation of the SCORPIO spectra with the OSIRIS one shows small velocity differences of $8.4 \pm 6.6\,\mathrm{km\,s^{-1}}$ and $-10 \pm 14\,\mathrm{km\,s^{-1}}$ for Feb 21 and 22 respectively. All uncertainties are 1σ equivalent.

Using the task FITSPEC in the STSDAS SYNPHOT[3] and template spectra from Jacoby et al. (1984), Sánchez-Blázquez et al. (2006) and Le Borgne et al. (2003) we fitted our spectra in an attempt to estimate the reddening. Fitting the spectrum on Jan 15 with a F5I template we obtained a reddening $E_{\mathrm{B-V}} = 0.37$ mag. For the spectrum on Jan 21 fitted with a F0I template the corresponding $E_{\mathrm{B-V}}$ was 0.33 mag. Merged spectra on Feb 21 and 22 and the spectrum on Feb 24 were best fitted with a K3I template and $E_{\mathrm{B-V}} = 0.25$ mag and $E_{\mathrm{B-V}} = 0.42$ mag respectively.

Combining the column hydrogen densities of Nieten et al. (2006) with the gas-to-dust (Nedialkov et al. 2011) ratio yields total color excess on the line of sight $E_{B-V} = 0.44 \pm 0.08$ mag. An identical result: $E_{B-V} = 0.42 \pm 0.03$ mag is derived from the maps of the M31 dust surface density (Draine et al. 2014). A comparison of the $B-V$ and $V-R$ colors with the catalog com-

[3] STSDAS is a product of the Space Telescope Science Institute, which is operated by AURA for NASA.

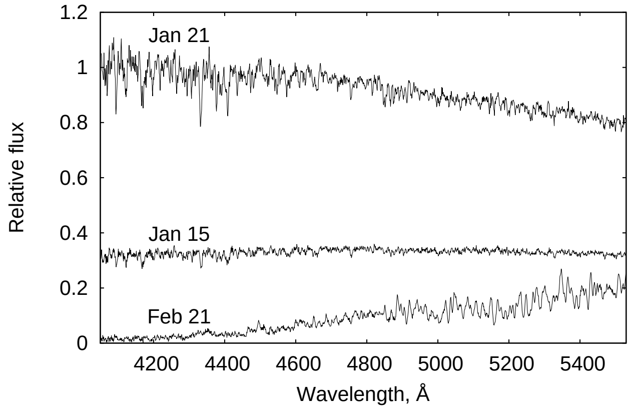

Fig. 3. BTA/SCORPIO spectra obtained with the VPHG1200B and G grisms. The Jan 21 spectrum is close to maximum brightness and arbitrary shifted to unity. The relative flux and shape of the Jan 15 and Feb 21 spectra reflect the evolution of the luminosity and the colors.

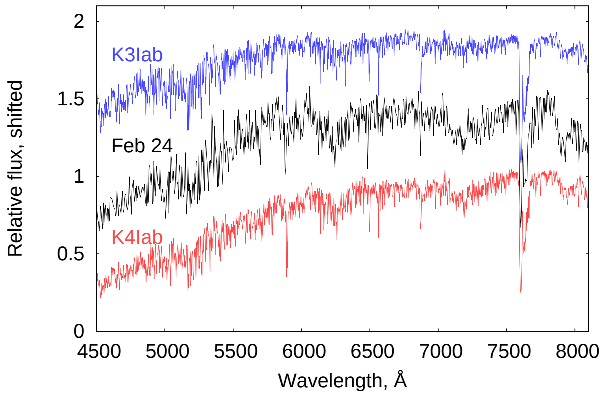

Fig. 4. The combined GTC/OSIRIS spectrum dereddened by E_{B-V} = 0.4 mag in comparison to HD 157999 (K3Iab) and 41 Gem (K4Iab).

piled by Worthey & Lee (2011) shows that the reddening E_{B-V} is in the range of 0.15 – 0.58 mag. The mean reddening value, obtained from the spectra – $E_{B-V} = 0.35 \pm 0.10$ mag, of which ~0.05 mag can be attributed to the interstellar reddening in our Galaxy (Schlafly & Finkbeiner 2011), is well within this range. It suggests a true color of $(B-V)_0 = 0.15 \pm 0.10$ mag and a V-band bolometric correction of +0.03 mag at maximum. Adopting a distance modulus $(m - M) = 24.47$ mag[4] and a total-to-selective extinction $R_V = 3.1$ yields a peak absolute magnitude $M_V = -10.13 \pm 0.30$ mag. This sets the luminosity limits at maximum on $L_{bol} = 8.7^{+3.3}_{-2.2} \times 10^5 L_\odot$. Note, that M31N 2015-01a is projected inside a tiny (2″x2″) HII region #1527 (Azimlu et al. 2011). The latter list an extinction $A_R = 0.538$ mag, which corresponds to the somewhat lower $E_{B-V} = 0.23$ mag. An association with this HII region could decrease the luminosity estimate to $\sim 6 \times 10^5 L_\odot$.

4. Summary

The outburst of M31N 2015-01a was a very luminous event, reaching $\sim 10^6 L_\odot$ at the optical maximum. We present accurate photometry and astrometry in the period January-March 2015. The transient shares all major observational characteristics of red novae and we conclude that it belongs to this group of events. The fading was slow at first with $t_2 \sim 50\,d$ in R-band. In a one-month period $B-R$ increased by 2.1 mag and the observed spectral type changed from F0I to K3I. The exploration of red novae is so far based on a very small sample of sources, which makes M31N 2015-01a so important: it moves us a step closer to recognizing similarities and differences in their behaviour.

[4] The NED database (`http://ned.ipac.caltech.edu/`) lists a median $(m - M) = 24.45$ mag for M31. If the object lies in the M31 plane, its location suggests a +0.02 mag difference from the center.

Acknowledgements. This work was partially financed by grant No. BG051 PO001-3.3.06-0057 of the European Social Fund. Based on observations made with the GTC telescope, in the Spanish Observatorio del Roque de los Muchachos of the Instituto de Astrofísica de Canarias, under Director's Discretionary Time. Also based on observations made with the Nordic Optical Telescope at the Observatorio del Roque de los Muchachos. This work makes use of observations from the LCOGT network. KH was supported by the project RVO:67985815. AK&EO gratefully acknowledge observing grant support from the Institute of Astronomy and Rozhen National Astronomical Observatory, Bulgarian Academy of Sciences. KV acknowledges support from the Hungarian Research Grant OTKA K-109276, OTKA K-113117 and the "Lendület" Program (LP2012-31) of the Hungarian Academy of Sciences. KV, KS and LM have been supported by the Lendület-2009 program of the Hungarian Academy of Sciences and the ESA PECS Contract No. 4000110889/14/NL/NDe. EAB and VPG thank the Russian Foundation for Basic Research for the financial support by Grant 14-02-00759. The research was supported by the Russian Scientific Foundation (grant N 14-50-00043). SF acknowledges support of the Russian Government Program of Competitive Growth of Kazan Federal University. AWS acknowledges support from NSF grant AST1009566. We thank to H. Kučáková, J. Vraštil and M. Wolf for obtaining images at Ondřejov.

References

Afanasiev, V. L. & Moiseev, A. V. 2005, Astronomy Letters, 31, 194
Azimlu, M., Marciniak, R., & Barmby, P. 2011, AJ, 142, 139
Bond, H. E., Henden, A., Levay, Z. G., et al. 2003, Nature, 422, 405
Cepa, J. 1998, Ap&SS, 263, 369
Dong, S., Kochanek, C. S., Adams, S., & Prieto, J.-L. 2015, ATel, 7173, 1
Draine, B. T., Aniano, G., Krause, O., et al. 2014, ApJ, 780, 172
Evans, A., Geballe, T. R., Rushton, M. T., et al. 2003, MNRAS, 343, 1054
Fabrika, S., Barsukova, E. A., Valeev, A. F., et al. 2015, ATel, 6985, 1
Goranskij, V. P., Cherjasov, D. V., Safonov, B. S., et al. 2015, ATel, 7206, 1
Hamuy, M., Suntzeff, N. B., Heathcote, S. R., et al. 1994, PASP, 106, 566
Hamuy, M., Walker, A. R., Suntzeff, N. B., et al. 1992, PASP, 104, 533
Hodgkin, S. T., Campbell, H., Fraser, M., et al. 2015, ATel, 6952, 1
Jacoby, G. H., Hunter, D. A., & Christian, C. A. 1984, ApJS, 56, 257
Jockers, K., Credner, T., Bonev, T., et al. 2000, Kinematika i Fizika Nebesnykh Tel Supplement, 3, 13
Kaminski, T., Menten, K. M., Tylenda, R., et al. 2015, ArXiv e-prints [arXiv:1503.06570]
Kochanek, C. S., Adams, S. M., & Belczynski, K. 2014, MNRAS, 443, 1319
Kulkarni, S. R., Ofek, E. O., Rau, A., et al. 2007, Nature, 447, 458
Kurtenkov, A., Ovcharov, E., Nedialkov, P., et al. 2015a, ATel, 6941, 1
Kurtenkov, A., Tomov, T., Fabrika, S., et al. 2015b, ATel, 7150, 1
Le Borgne, J.-F., Bruzual, G., Pelló, R., et al. 2003, A&A, 402, 433
Magnier, E. A., Lewin, W. H. G., van Paradijs, J., et al. 1992, A&AS, 96, 379
Martini, P., Wagner, R. M., Tomaney, A., et al. 1999, AJ, 118, 1034
Mason, E., Diaz, M., Williams, R. E., Preston, G., & Bensby, T. 2010, A&A, 516, A108
Massey, P., Olsen, K. A. G., Hodge, P. W., et al. 2006, AJ, 131, 2478
Munari, U., Henden, A., Kiyota, S., et al. 2002, A&A, 389, L51
Nedialkov, P., Williams, B., Green, J., & Hatzidimitriou, D. 2011, in AIP Conference Series, Vol. 1356, AIP Conference Series, ed. I. Zhelyazkov & T. Mishonov, 45–49
Nieten, C., Neininger, N., Guélin, M., et al. 2006, A&A, 453, 459
Oke, J. B. 1990, AJ, 99, 1621
Rau, A., Kulkarni, S. R., Ofek, E. O., & Yan, L. 2007, ApJ, 659, 1536
Rich, R. M., Mould, J., Picard, A., Frogel, J. A., & Davies, R. 1989, ApJ, 341, L51
Roeser, S., Demleitner, M., & Schilbach, E. 2010, AJ, 139, 2440
Sánchez-Blázquez, P., Peletier, R. F., Jiménez-Vicente, J., et al. 2006, MNRAS, 371, 703
Schlafly, E. F. & Finkbeiner, D. P. 2011, ApJ, 737, 103
Shumkov, V., Lipunov, V., Gorbovskoy, E., et al. 2015, ATel, 6911, 1
Sparks, W. B., Bond, H. E., Cracraft, M., et al. 2008, AJ, 135, 605
Tylenda, R., Hajduk, M., Kamiński, T., et al. 2011, A&A, 528, A114
Tylenda, R. & Soker, N. 2006, A&A, 451, 223
Williams, S. C., Darnley, M. J., Bode, M. F., & Steele, I. A. 2015, ArXiv e-prints [arXiv:1504.07747]
Worthey, G. & Lee, H.-c. 2011, ApJS, 193, 1

Table 4. Calculated magnitudes for M31N 2015-01a in Johnson-Cousins *BVRI* filters.

JD-2457000	filter	mag	err	telescope	airmass
36.264	B	19.641	0.161	RSCH	1.17
38.248	B	17.046	0.017	BTA	1.30
38.345	B	16.992	0.029	RSCH	1.69
39.261	B	16.549	0.017	RSCH	1.19
39.413	B	16.498	0.029	UL50	1.53
40.295	B	16.215	0.017	RSCH	1.35
44.196	B	15.934	0.017	BTA	1.16
46.612	B	16.109	0.026	LCOGT	1.32
48.658	B	16.679	0.242	LCOGT	1.71
51.611	B	17.261	0.026	LCOGT	1.38
60.323	B	17.865	0.096	KSCH	1.79
61.252	B	17.974	0.026	KSCH	1.32
67.257	B	18.294	0.066	KSCH	1.42
68.246	B	18.383	0.022	RSCH	1.53
72.249	B	18.719	0.103	KSCH	1.46
75.224	B	18.791	0.018	BTA	1.92
93.340	B	20.076	0.051	NOT	2.53
96.346	B	20.385	0.041	NOT	2.99
38.246	V	16.416	0.008	BTA	1.29
44.187	V	15.436	0.011	BTA	1.14
66.319	V	16.626	0.012	KSCH	1.93
67.243	V	16.621	0.026	KSCH	1.35
72.241	V	16.832	0.065	KSCH	1.41
75.225	V	16.873	0.013	BTA	1.93
89.323	V	17.869	0.059	UL50	1.92
92.246	V	18.098	0.108	KSCH	1.91
36.243	R	18.087	0.026	RSCH	1.11
37.210	R	17.213	0.011	R2M	1.05
38.246	R	16.051	0.011	BTA	1.29
38.330	R	16.047	0.009	RSCH	1.55
39.242	R	15.679	0.009	RSCH	1.13
40.283	R	15.407	0.009	RSCH	1.29
40.390	R	15.364	0.012	R2M	2.38
44.189	R	15.133	0.011	BTA	1.14
46.617	R	15.165	0.013	LCOGT	1.34
48.661	R	15.347	0.032	LCOGT	1.75
51.615	R	15.609	0.011	LCOGT	1.41
57.285	R	15.678	0.011	ONDR	1.36
59.238	R	15.692	0.011	ONDR	1.20
60.317	R	15.675	0.012	KSCH	1.73
61.234	R	15.683	0.011	KSCH	1.24
62.596	R	15.681	0.009	LCOGT	1.50
64.608	R	15.689	0.009	LCOGT	1.66
66.310	R	15.725	0.011	KSCH	1.82
67.239	R	15.741	0.009	KSCH	1.33
68.230	R	15.804	0.013	RSCH	1.42
72.244	R	15.839	0.027	KSCH	1.42
73.250	R	15.858	0.009	ONDR	1.40
75.223	R	15.894	0.024	BTA	1.90
80.270	R	16.111	0.011	ONDR	1.68
86.329	R	16.417	0.021	ONDR	2.72
87.302	R	16.437	0.016	ONDR	2.28
89.266	R	16.642	0.012	ONDR	1.88
89.337	R	16.617	0.061	UL50	2.08
92.245	R	16.987	0.104	KSCH	1.90
93.345	R	17.011	0.011	NOT	2.68
96.351	R	17.315	0.013	NOT	3.19
99.283	R	17.617	0.035	ONDR	2.54
105.279	R	18.499	0.084	ONDR	2.79
60.320	I	15.028	0.021	KSCH	1.76
61.245	I	15.017	0.018	KSCH	1.28
67.241	I	15.019	0.018	KSCH	1.34
68.272	I	15.085	0.016	RSCH	1.78
72.246	I	15.048	0.028	KSCH	1.44
89.357	I	15.344	0.111	UL50	2.34
92.248	I	15.377	0.065	KSCH	1.92
93.350	I	15.557	0.021	NOT	2.84
96.356	I	15.735	0.021	NOT	3.42